Heliyon 10 (2024) e36946

Contents lists available at ScienceDirect

Heliyon

journal homepage: www.cell.com/heliyon

Research article

A comparative thermo-chemical characterization of oilseed, millet and pulse stem biomass for bioethanol production

Spandan Nanda [a,***], Abinash Mishra [a], Amrita Priyadarsini [a], Tanya Barpanda [a], Amiya Kumar Baral [a], Supriya Jena [a], Pradip Kumar Jena [a,**], Bipranarayan Mallick [b], Manasi Dash [a,*], Nandita Swain [a], Nitish Kumar Jena [c], Mahendra Kumar Mohanty [a]

[a] Odisha University of Agriculture & Technology, Bhubaneswar, Odisha, India
[b] Model Degree College, Rayagada, Odisha, India
[c] Tamil Nadu Agricultural University, Coimbatore, India

ARTICLE INFO

Keywords:
Agri-wastes
Feedstock
TGA
Spectroscopy
ICP-OES
Bioethanol

ABSTRACT

Various thermochemical and biochemical processes are resorted to transform agri-wastes into diverse green fuels. Current investigation encompassed three different types of biomass *viz.*, gingelly, kodo millet and horse grams, whose desirability as biofuel feedstock have been largely unexplored till date. The existence of significant amount of cellulose (38.07 %), volatiles (75.19 %), calorific value (avg. 16.98 MJ/kg) in the gingelly biomass, demonstrates the effectiveness of the concerned biomass for utilization as feedstock in diverse industrial applications. The mean estimates of Eα were lower for kodo millet (approx. 150 kJ/mole), followed by gingelly (approx. 178 kJ/mole) and horse gram (approx. 180 kJ/mole). The mean estimates of ΔHα were 174.81 (FWO), 170.22 (KAS), 169.17 (S) and 170.40 (T) kJ/mol for the gingelly biomass. The mean estimates of ΔHα were 147.83 (FWO), 148.81 (KAS), 147.93 (S) and 149.04 (T) kJ/mol for kodo millet biomass, while for horse gram biomass, mean estimates of ΔHα were 178.91 (FWO), 169.61 (KAS), 168.56 (S) and 168.81 (T) kJ/mol. The minor difference of 3–4 kJ/mole between Aα and Hα, signifies the viability of the thermal disintegration process. From master plot, it's evident that the experimental curve intersects multiple theoretical curves, highlighting the intricate characteristics of the thermal disintegration process. The overall ethanol recovery was highest in gingelly as compared to both the biomasses. Gingelly biomass yielded an ethanol titer of 24.8 g/L after 24 h, resulting in a volumetric ethanol productivity of 1.03 g/L/h and an ethanol yield of 0.36 g/g.

1. Introduction

The rise in dependency on fossil fuels including petro-chemical substances, creates consequential and existential threat to both the

* Corresponding author.
** Corresponding author.
*** Corresponding author.
E-mail addresses: nanda.spandan56@gmail.com (S. Nanda), ampbg1996@gmail.com (A. Mishra), Pradip_callme@yahoo.co.in (P.K. Jena), mdpbgouat@gmail.com (M. Dash).

https://doi.org/10.1016/j.heliyon.2024.e36946
Received 6 April 2024; Received in revised form 20 August 2024; Accepted 25 August 2024
Available online 28 August 2024

environment and human being, respectively. The liberation of potential GHGs, like carbon dioxide, contributes to the amplification of global warming mechanisms, subsequently intensifying the occurrence of diverse natural disasters. Emerging economies like India are actively striving to identify potential alternatives to non-renewable fossil energy sources, with an aim to achieve self-sufficiency and reduce dependence on imported petroleum products. Hence, in order to deal with the twin issues i.e effective waste management and to reduce foreign expenditures, various biomasses have been analysed to their potentiality to be used as biofuel feedstock.

Various bio-chemical and thermo-chemical processes involving thermal disintegration of bio-wastes has been employed to convert the dry matters into desirable green fuels and related products. Significant researches are exploring the suitability of different biomasses to be employed as biofuel feedstocks. Such investigations have focused on few biomasses including straw of rice, little millet, sunflower stem, banana stalk, cob of maize, sorghum, jute, jackfruit seeds and coconut husk [1–10]. Thermogravimetry (TGA) is one of the principal methods of exploring the thermal disintegration properties of biomasses [11]. The key steps during thermal disintegration are *viz.*, i) elimination of water and volatile components from biomass, ii) disintegration of non-cellulosic polysaccharides, iii) disintegration of cellulose, and iv) disintegration of lignin. The composition of cell wall polymers in crops significantly influences the thermal disintegration characteristics. The primary (PCW) and secondary (SCW) cell wall are mostly composed of cellulosic fibrils, non-cellulosic polysaccharides and lignin. Several researches reported cellulose contents of 42 % in *Saccharum officinarum* bagasse, 32 % in rice straw, 38 % in maize stover and 29–35 % in *Triticum aestivum* straw.

Gingelly, also known as sesame, the queen of oilseed, is believed to have originated in sub-Saharan Africa while the cultivated type is thought to have originated in the Indian sub-continent. Besides its prominent use in Asian cuisine as vegetable oil, gingelly has diverse industrial applications, serving as a potential raw material for soaps, lubricants, cosmetics, pharmaceuticals, and animal feed [12]. India, contributing 40 % of global gingelly area and 27 % of production, is a key hub [13]. Post-harvest practices result in substantial biomass accumulation, largely unexplored for vital by-products like biofuels. While gingelly straw lacks palatability for domestic animals and isn't suitable for mushroom production, exploring its bioenergy potential from straw biomass remains untapped [14]. This approach will not only minimizes waste but also aids India in reducing petro-product imports while emphasizing on green fuel generation [14]. Millets, regarded as one of the earliest cultivated cereal grains, have been fundamental to the diets of communities in semi-arid regions of Asia and Africa for centuries due to their resilience in challenging climates. Classified into major (Sorghum, Pearl, Finger millet), minor (Foxtail, Kodo, Barnyard, Little, Proso millet), and pseudo-millets (Amaranth, Buckwheat millet), these grains have a rich history of cultivation in India, China, Malaysia, Srilanka, Australia, and parts of Africa. Originating in India, Kodo millet (Paspalum scrobiculatum L.) has been cultivated for approximately 3000 years, primarily in the Deccan plateau. This highly drought-tolerant crop, with significant untapped residue, holds promise for producing valuable bi-products, including green fuels [15]. Horse gram, belonging to the Fabaceae family, stands out as a promising grain legume with exceptional nutritional and remedial attributes, displaying resilience to harsh environmental conditions. Widely cultivated across the globe, particularly in East and Northeast Africa, India, China, Philippines, Bhutan, Pakistan, Sri Lanka, and Queensland, Australia, it constitutes 5–10 % of India's pulse production, with an annual output of approximately 0.65 million tons [16]. Recognized by the US National Academy of Sciences as a valuable food source for the future, horse gram serves as a nutrient-dense legume, addressing food and nutritional security for low-income communities in developing countries [17]. The cultivation residues of horse gram, much like those of kodo millet and gingelly, represent an underexplored resource for the production of valuable by-products, particularly in the realm of green fuels. In 2014, global sesame production reached 5.47 million tons, with Africa contributing 51 % (2.79 million tons) and the Nile Basin countries contributing 33 % (1.8 million tons) of the total output. Additionally, the worldwide biomass production of pulses stands at approximately 50 million tons. Meanwhile, in India, millet cultivation occupies an estimated total area of 84 million hectares, yielding around 10.23 million metric tonnes (MMT) – approximately 41 % of the global production according to FAO (2019). This comprehensive exploration of diverse agricultural by-products for sustainable energy sources will supplement the broader goal of reducing the negative environmental impact leading to more resilient and resource-efficient agricultural landscape. Hence, as discussed above TGA is highly rewarding in terms of deciphering the bioenergy potential of various feed stocks [18–21]. Considering these situations, in the present investigation, stem biomass of gingelly, kodo millet and horse gram were used to estimate the kinetics as well as thermodynamic parameters to explore the possibilities of their utilization as feed stock in the thermochemical conversion. These biomasses were also subjected to a plethora of biochemical, elemental and spectroscopic characterization to decipher their potential to be used as desirable feedstock.

2. Materials and methods

2.1. Biomass Sample processing

Fresh stem biomasses were collected after harvesting of the concerned crops, cultivated in the experimental blocks of OUAT, Odisha, India. Initially, samples free from insect pest and diseases, were washed thoroughly with distilled water. The samples were then sun dried to decrease moisture content, followed by mechanical drying using a hot air oven (Scientech, India). Subsequently, the dried biomass with lowered moisture levels was pulverized to a fine powder of particle size of 212 μm.

2.2. Comprehensive chemical and Elemental Profiling

NREL protocols were followed for proximate analysis of the biomasses in order to estimate the volatiles, bound water and ash levels. The biochemical assay was performed by employing HP-Liquid Chromatography (Aminex HPX- 87H column-Shimadzu, Japan). The determination of fixed carbon content was achieved through the mathematical formula *i.e.,* FC (%) = 100%-(bound water +

volatiles content + ash)%. Elemental Profiling of the biomasses which includes carbon(C), nitrogen(N), oxygen(O), & sulphur(S) was done utilizing an Elemental Analyzer (ELEMENTAR, UNICUBE, Germany). The calorific value assessment for stem samples was conducted using a Bomb Calorimeter (C 3000, IKA, Germany). The acid soluble fraction of lignin polymer was determined with the aid of an UV–VIS spectrophotometer (PerkinElmer, Lambda 365, USA) and by following NREL protocol. The elemental composition of ash of biomass sample was determined using inductively coupled plasma optical emission spectroscopy ICP-OES (PerkinElmer, USA). The FTIR spectra was generated employing the FTIR spectroscopy (PerkinElmer, USA).

2.3. Thermal characterization (TGA/DTG)

Thermogravimetry of stem biomasses was performed through a TGA analyser (Hitachi STA 7200, Japan). Four heating rates from 5 to 20 °C min^{-1} were used under current investigation. Temperature starting from 30 °C to 800 °C was considered for TGA analysis, as bulk of PCW and SCW wall complexes such as cellulose and non-cellulosic polysaccharides, went on thermal disintegration under such temperal regime. Present investigation included 11 mg of 212μ sample to analyse the desirability of the concerned biomass with respect to industrial feedstock capability.

2.4. Kinetic analysis

The universal pyrolysis rate reaction during the decomposition of biomass is given by,

$$\frac{d\alpha}{dt} = k(T) * f(\alpha) \tag{1}$$

Where, dα/dt is referred as the conversion with time, f(α) is the method referring the change in physio-chemical characteristics. The conversion rate (α) of biomass is given by,

$$\alpha = \frac{w_{initial} - w_{instntaneous}}{w_{initial} - w_{residual}} \tag{2}$$

From Eq. (1), and by using the fundamental kinetic equation i.e the Arrhenius equation, the integral from of conversion [G(α)] is given by,

$$G(\alpha) = \int_0^{\alpha} \frac{d\alpha}{f(\alpha)} = \int_0^{T} \frac{A}{\beta} e^{\frac{-E_\alpha}{RT}} dT = \frac{AE_\alpha}{\beta R} P(X) \tag{3}$$

Where, E_α is the activation energy of the biomass at a fixed conversion α, A is the pre-exponential factor, R is the universal gas constant, β is the heating rate of the biomass complex, P(X) is the temperature integral function. In the present investigation, different model-free isoconversional methods such as Flynn wall Ozawa (FWO), Kissinger Akahira Sunose (KAS), Starink (S) and Tang (T) are employed for the determination of apparent activation energy and the thermodynamics parameters. These methods are more robust as compared to non-isoconversional method such as Kissinger method.

2.4.1. Flynn wall Ozawa (FWO) method

The E_α and A were determined by using the following Eq. (4) under FWO [22].

$$\ln \beta = \ln\left(\frac{AE_\alpha}{g(\alpha)R}\right) - 5.331 - 1.052\left(\frac{E_\alpha}{RT}\right) \tag{4}$$

Here, from the plot between ln β vs 1/T at different level of α, the slope ($-E_\alpha/R$) and intercept [$\ln(A\,E_\alpha/g(\alpha)R$] were estimated.

2.4.2. Kissinger Akahira Sunose (KAS) method

The E_α and A were determined by using the following Eq. (5) under KAS [23].

$$\ln\left(\frac{\beta}{T^2}\right) = \ln\left(\frac{AR}{E_\alpha g(\alpha)}\right) - \frac{E_\alpha}{RT} \tag{5}$$

Here, the plot between ln β/T^2 vs 1/T at different level of α, provided the slope ($-E_\alpha/R$) and intercept [$\ln(AR/g(\alpha)\,E_\alpha$].

2.4.3. Starink (S) method

The following Eq. (6) was employed to estimate the kinetics parameters under the Starink method.

$$\ln\left(\frac{\beta}{T^{1.92}}\right) = \text{Constant} - 1.008\left(\frac{E_\alpha}{RT}\right) \tag{6}$$

The plot of $\ln(\beta/T^{1.92})$ vs 1/T estimated slope as −1.008 (E_α/R) [24].

2.4.4. Tang (T)method

The following Eq. (7) was used to estimate the kinetics parameters under the Tang method.

$$\ln\left\{\frac{\beta}{T^{1.89466100}}\right\} = \text{Constant-}\ 1.001145033\left(\frac{E_\alpha}{RT}\right) \tag{7}$$

The plot of $\ln(\beta/T^{1.89466100})$ vs 1/T estimated slope as −1.00145033 (E_α/R) [25].

2.4.5. Estimation of thermodynamic parameters

The thermodynamic parameters, viz. ΔH, ΔG and ΔS were calculated using Eqs. (8)–(10) as follows [26].

$$\Delta H = E_\alpha\text{-}RT \tag{8}$$

$$\Delta G = E_\alpha + R\ T_m\ \ln\left(\frac{K_b * T_m}{hA}\right) \tag{9}$$

$$\Delta S = \frac{\Delta H\text{-}\Delta G}{T_m} \tag{10}$$

Where, K_b is the Boltzmann constant ($1.38064852 \times 10^{-23}$ m^2 kg s^{-2} K^{-1}) and h is the planks constant ($6.62607004 \times 10^{-34}$ m^2 kg s^{-1}).

2.4.6. Z(α)-master plots (model-free method)

The predictions made by master plots are more robust as compared to linear fitting model i.e Coats-Redfern analyses. Theoretical (Eq. (11)) and experimental master plots (Eq. (12)) are compared to arrive at the appropriate reaction mechanism controlling the complex pyrolysis process of the rice biomass. For theoretical master plots several solid-state functions are listed in the Supplementary Table 1 [9],.

$$Z(\alpha) = f(\alpha) * g(\alpha) \tag{11}$$

$$Z(\alpha) = \frac{d\alpha}{dt} * \exp\left(\frac{E_\alpha}{RT_\alpha}\right) \int_0^{T_\alpha} \exp\left(\frac{E_\alpha}{RT_\alpha}\right) \tag{12}$$

2.5. Ethanol production in a laboratory bioreactor via SSF

The scaled-up simultaneous saccharification and fermentation (SSF) experiments utilized microwave-alkali acid pre-treated stem biomasses as a substrate in a 3-L thermostatically controlled glass reactor (Model: BioSpin-03 A, Bio-Age Equipments Pvt. Ltd, Mohali, India). Following the optimized conditions from run 2 [substrate loading: 11 % (w/v), pH: 4.5, temperature: 30 °C, enzyme loading: 0.5 % (v/v), and inoculum size: 8 % (v/v)] determined by Taguchi design, the SSF experiments were conducted for 72 h. The bioreactor vessel, containing microwave-alkali-acid pre-treated stem biomasses, was supplemented with the same nutrient solution used in shake-flask SSF. Prior to the addition of the cellulase cocktail and ethanologenic yeast, it underwent autoclave sterilization (121 °C, 15 lbs) for 15 min. Maintaining a pH of 4.5, a 5 N NaOH solution was employed, with constant agitation at 120 rpm. Samples were withdrawn at 12-h intervals up to 72 h for ethanol estimation.

3. Results and discussion

3.1. Proximate ultimate & biochemical profiling

The diverse constituents of the three types of stem biomass were subjected to meticulous scrutiny (Table 1). Notably, the gingelly, kodo millet and horse gram biomass exhibited comparably diminished moisture content, rendering them well-suited feedstock for thermal disintegration processes. The volatile matter composition was quantified as 75.19 % for gingelly, 79.38 % for kodo millet, and 76.46 % for horse gram, a pivotal attribute requisite for a proficient feedstock composition. Concomitantly, the quantity of ash content was quantified as 7.62 %, 7.89 %, and 7.77 % for gingelly, kodo millet, and horse gram, respectively. The observed lower ash content is consequential in light of its known adverse influence on the conversion process, thereby rendering these biomass samples particularly advantageous in this regard. The carbon content in ranged between 36.3 % and 38.3 %, while the hydrogen varied from 4.95 % to 5.2 %. All the three-stem biomass had a limited amount of sulphur and nitrogen (0.30–1.15 %). The presence of oxygen content was observed in the range of 55.50 %–57.22 %, which results in high volatile matter. Additionally, calorific value (HHV), a pivotal indicator of feedstock quality, was notably prominent, registering at 16.98 MJ/kg (gingelly), 16.43 MJ/kg (kodo millet), and 17.34 MJ/kg (horse gram), a common trait shared among various lignocellulosic biomasses. In terms of cellulose content, gingelly emerged as preeminent with 38.07 %, followed by horse gram with 36.05 %, and kodo millet with 35.05 %. Bio polymeric composition, notably cellulosic microfibrils, creates a distinct impact on the kinetic appraisals of the dry matter under investigation. This is corresponding with the distinct accumulation of cellulose (average 36.39 %), volatiles (average 77.01 %), and HHV(high heating value) (average

Table 1
Proximate ultimate & biochemical profiling.

Biomass sample	Proximate analyses (wt%)				Ultimate analyses (wt%)					Calorific value (MJ/Kg)	Cell wall component (%)		
	Moisture content	volatile matter	Ash content	Fixed carbon	C	H	O*	N	S		Cellulose	Hemicellulose	Total Lignin
Gingelly	8.14	75.19	7.62	9.05	36.31	5.01	57.22	1.13	0.33	16.98	38.07	12.63	18.19
Kodo millet	7.51	79.38	7.89	5.22	36.53	4.98	57.03	1.15	0.31	16.43	35.05	10.19	17.36
Horse gram	8.34	76.46	7.77	7.43	38.22	5.17	55.50	0.84	0.27	17.34	36.05	11.5	18.98

16.91 MJ/kg) across the entire spectrum of investigated biomasses, thereby affirming their favourable suitability for the pyrolysis process of ethanol production (Table 1).

3.2. Elemental Profiling

Table 2 provides the elemental composition of ash derived from the stem biomass samples. During the biofuel production process, it has been observed that metal cations play a significant role in influencing enzymatic processes. Specifically, Ca^{2+} and Mg^{2+} have been noted to enhance catalytic activity, while K^{+} inhibits the catalytic activity of the β-Glucosidase enzyme. Sesame exhibited the highest percentages of calcium (4.35 ppm) and magnesium (1.82 ppm) followed by kodo millet and horse gram, suggesting its suitability as a promising feedstock for bioethanol production. The accumulation of these elements in plant biomass occurs through nutrient absorption from soil and water, leading to ash formation. Notably, horse gram exhibited the highest silica (4.2 ppm) content among the three biomass types followed by kodo millet (3.8 ppm) and gingelly (2.8 ppm). Binod and co-workers have previously reported that elevated ash levels contribute to increased silica content in biomass [27]. Biomass possessing lower silica level is more desirable for bioethanol production. Gingelly was found to possess least amount of silica compared to other two counterparts, indicating its potentiality for a desirable feed stock (see Fig. 2).

3.3. FTIR analysis

A comprehensive spectroscopic investigation was carried out to discern the chemical moieties present in biomolecules, with the primary objective of discerning the principal constituents of the cell wall across distinct sections of the gingelly, kodo millet & horse gram. Employing Fourier-transform infrared (FTIR) spectroscopy spanning the wavenumber range of 400–4000 cm^{-1}, conspicuous peaks in Fig. 3 emerged at 3325, 3341, and 3283 cm^{-1} for the gingelly, kodo millet and horsegram, respectively. These peaks signify O-H stretching vibrations, providing strong evidence for the presence of O-H and C_6H_5 groups, characteristic of heterogeneous aromatic polymer [28]. Further spectral characteristics emerged at 2925, 2920, and 2924 cm^{-1}, alongside 1734, 1737, and 1742 cm^{-1} for the gingelly, kodo millet and horsegram, corresponding to C-H stretching vibrations [29]. These vibrations are linked to the CH_2 and CH_3 groups present in heterogeneous aromatic polymer, along with CO stretching vibrations, which validate the existence of CHO, >C=O, and aliphatic ester groups, recognized features of the afore mentioned components. Affirmation of heterogeneous aromatic polymer's presence was confirmed by absorbance bands at 1625, 1516, and 1417 cm^{-1} within the gingelly, and at 1616, 1507, and 1447 cm^{-1} in the kodo millet, as well as 1646 cm^{-1} and 1433 cm^{-1} in the horse gram. These bands resonate with carbonyl stretching vibrations in aromatics, C=C stretching vibrations within the aromatic ring, and H-C plane deformation, respectively, reinforcing the indication of heterogeneous aromatic polymer [30]. Confirmation of the existence of heteropolysaccharides and cellulose was attained through the identification of H-C bending and H_2C wagging vibrations at 1365 cm^{-1} and 1327 cm^{-1}, respectively. Additionally, the characteristic aromatic ring vibration attributed to heterogeneous aromatic polymer was observed at 1245 cm^{-1} [31]. Further verification of the presence of the primary cell wall polymers was substantiated by the carbonyl, and C-O-C stretching band at 1024 cm^{-1}. An indication of glycosidic linkages, a marker of the hemicellulose polymer, was observed at 764 cm^{-1}. A broad peak at 3300-3500 cm^{-1} corresponding to O-H stretching vibrations indicates the presence of cellulose in the three biomass samples. The gingelly biomass yields a broad peak of higher intensities at the concerned wavelength range as compared to other two biomasses. Also, gingelly exhibited highest cellulose accumulation along with highest ethanol recovery as compared to other biomasses.

3.4. Thermal breakdown properties analysis

Thermal disintegration property of biomasses was explored by employing thermo-gravimetric analysis. A temperal range from 30 °C to 800 °C was used under current investigation. The pictorial representations (Fig. 1a and b) depict characteristics disintegration pattern of three different types of biomasses under different temperal regions (Table 3). Three characteristics sectors/regions can be seen in the TG and DTG curves and are referred as the sectors of moisture and volatiles removal (Sector 1), thermal disintegration of cellulose and hemicellulose (Sector 2) and disintegration of complex lignin (Sector 3). In the first sector, a 10 % weight loss was recorded in all the three types of biomasses. This weight loss percent is typically attributed due to vaporization of several cell-bound and surface water in addition to certain volatiles. This phenomenon was observed in DTG profiles as a minute characteristic loop (swelling). This was observed at a thermal range of about 31.16 °C to 185.73 °C (gingelly), 29.13 °C to 175.77 °C (kodo) and 31.07 °C to 165.94 °C (horse gram). Similar observations were made in castor [26], Sorghum [5], pearl millet, sunflower [2], finger millet [32] and pearl millet [33]. In the next thermal sector (sector 2), the weight loss (WL%) was approximately 50 % in gingelly, 51 % in kodo and 51 % in horse gram. In the DTG curves, a loop was observed in between 185.73 °C to 279.09 °C, 175.77 °C to 270.23 °C and 165.94 °C to 263.70 °C corresponding to degradation of hemicellulose in gingelly, kodo and horse gram, respectively. Another loop

Table 2
Elemental Profiling of Ash samples of three different biomasses (in ppm).

Biomass	Al	Ca	Cu	Fe	K	Mg	Mn	Na	Zn	P	Si
Gingelly	0.03	4.35	0.15	0.35	0.23	1.82	0.57	0.15	0.22	2.4	2.8
Kodo Millet	0.07	3.83	0.07	0.22	0.47	0.69	0.72	0.17	0.12	3.5	3.8
Horse gram	0.04	1.51	0.03	0.17	0.33	0.53	0.43	0.13	0.21	3.9	4.2

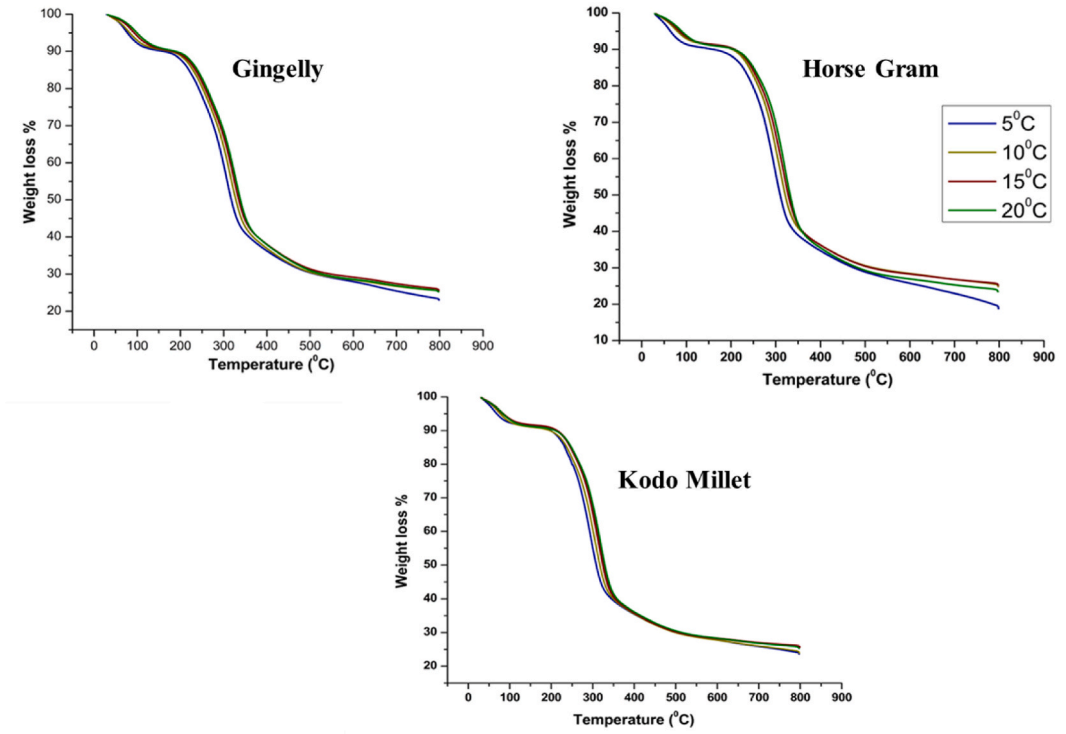

Fig. 1a. TG curves of stem biomasses.

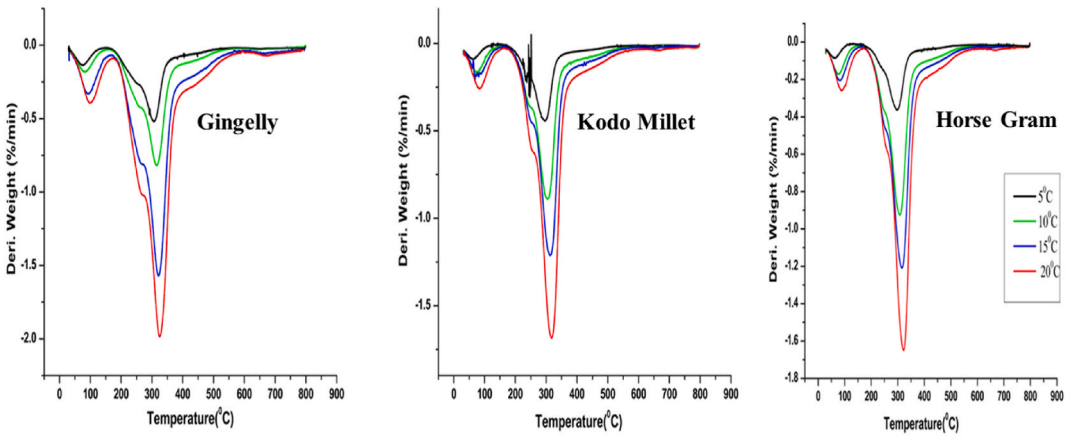

Fig. 1b. DTG curves of stem biomasses.

observed in between 281.36 °C to 373.55 °C (gingelly), 273.77 °C to 362.41 °C (kodo) and 265.31 °C to 366.28 °C (horse gram) was ascribed due to the disintegration of cellulose. Similar findings have been reported for orange, hazelnut, sorghum, finger millet, pearl millet, soyabean and maize cob [9,32–35]. In the third sector, the WL% was about 16.35 % (gingelly), 20 % (kodo) and 15.75 % (horse gram). Lignin, being a complex molecule, necessitates significant heat input to disintegrate in comparison to the other cell wall polymers. None of the loops or characteristic swelling was observed in the last distinguished sector. Hence, it has been characterized as passive pyrolysis sector or, chars generation sector. In the three types of biomasses, it was noticed that under each temperal sectors, the WL% declines with the change in "β" from 5 to 20 °C/min. This characteristic event has been described as "thermal lag" [36].

Scientific studies on the effect of heating rate are very crucial as it disseminates various key information on conversion, product distribution and the reactors to be used in the pyrolysis process [37]. With the increase in temperature, the conversion level of biomass rises (Supplementary Fig. 1). The Tm (temperature of maximum degradation of biomass) was reported as 306.83 °C, 316.41 °C, 321.66 °C and 325.62 °C under different heating rate of 5 °C/min, 10 °C/min, 15 °C/min and 20 °C/min, respectively for gingelly. The negative DTG loops was seen moving to right wards in the pictorial representations with the rise in heating rate. In gingelly, the range

Table 3
Degradation pattern of stem biomasses under different temperal regions.

Biomass type	Heating Rate (^{0}C/min)	Region-I			Region-II				Region-III		
		T_i	T_f	WL%	T_i	T_f	T_m	WL%	T_i	T_f	WL%
Gingelly	5	RT	181.34	8.88	181.34	369.44	306.83	44.45	369.44	800	10.02
	10	RT	185.73	9.88	185.73	373.55	316.41	50.18	373.55	800	13.25
	15	RT	199.35	9.10	199.35	381.22	321.66	47.68	381.22	800	10.11
	20	RT	207.39	9.22	207.39	392.43	325.62	49.34	392.43	800	9.90
Kodo millet	5	RT	172.34	10.21	172.34	318.34	318.44	47.84	318.34	800	14.09
	10	RT	175.77	9.61	175.77	362.41	327.44	51.21	362.41	800	20.02
	15	RT	208.31	10.02	208.31	372.56	340.01	51.34	372.56	800	12.34
	20	RT	209.78	9.99	209.78	380.09	343.34	51.36	380.09	800	13.11
Horse gram	5	RT	160.76	10.86	160.76	350.67	315.26	45.44	350.67	800	13.98
	10	RT	165.94	9.98	165.94	366.28	326.26	51.34	366.28	800	15.75
	15	RT	178.45	10.03	178.45	380.89	333.45	50.24	380.89	800	14.46
	20	RT	189.34	10.01	189.34	399.12	338.24	51.05	399.12	800	13.25

Where.
RT = Reaction temperature; T_i= Initial temperature; T_f = Final temperature; WL% = Weight loss%; T_m = Maximum thermal degradation temperature.

of reaction rate of disintegration as well as the concerned temperature were escalated from 0.51 % min^{-1} (306.83 °C) - 1.98 % min^{-1} (325.62 °C), in kodo, from 0.36 % min^{-1} (294.44 °C) - 1.64 % min^{-1} (323.09 °C) and for horse gram, from 0.44 % min^{-1} (297.06 °C) - 1.68 % min^{-1} (319.94 °C) with the increase in heating rate. On that account, it can be concluded, increased heating rate escalates reaction rate causing persistent rise in DTG curves in conjunction with the escalation in Tm estimate. Equivalent observations were made castor [26,38], Sorghum [5], little millet, sunflower [2], finger millet [32], ground nut shell [39,] pearl millet [33].

3.5. Thermal kinetic analysis

The international agency, ICTAC has recommended the use of robust iso-conversional models for estimation of activation energy and pre-exponential factors [40]. A wide range of conversion starting from 15 to 85 % of biomass was considered in order to have a greater insight into thermal disintegration process. The analytical data generated by employing suitable mathematical equations **(Eqs. (1)–(7))** and approximations are plotted in form of linear graphs (Fig. 2(a), (b), (c) and (d)) and were listed in Table 4. The Arrhenius plots thus generated under FWO, KAS, S and T, had clearly depicted the variations in apparent Eα with change in the conversion level. (see Fig. 2)As of now it is apparent that, biomass possessing significant level cellulose and hemicellulose, requires higher energy for thermal decay process. The Eα estimates for gingelly biomass was calculated as 179.39 kJ/mol (FWO), 180.98 kJ/mol (KAS), 179.85 kJ/mol (S) and 181.08 kJ/mol (T), for kodo millet biomass it was 152.42 kJ/mol (FWO), 155.27 kJ/mol (KAS), 153.98 kJ/mol (S) and 155.33 kJ/mol (T) and horse gram it was 183.48 kJ/mol (FWO), 179.76 kJ/mol (KAS), 185.54 kJ/mol(S) and 186.70 kJ/mol(T). Hence, it was observed that kodo millet biomass necessitates lowest level of energy input for thermal decay comparison to its other two biomass. For kodo biomass, with the "α" ranging from 0.15 to 0.75, the apparent estimates of Eα varied from 115.71 to 246.46 kJ/mol (FWO), 113.91–249.60 kJ/mol (KAS), 113.31–248.00 kJ/mol (S), 114.16–249.74 kJ/mol (T). This elevation in Eα estimates with corresponding rise in "α" was principally ascribed due to the higher energy requirements of the biomass in disintegration of the major

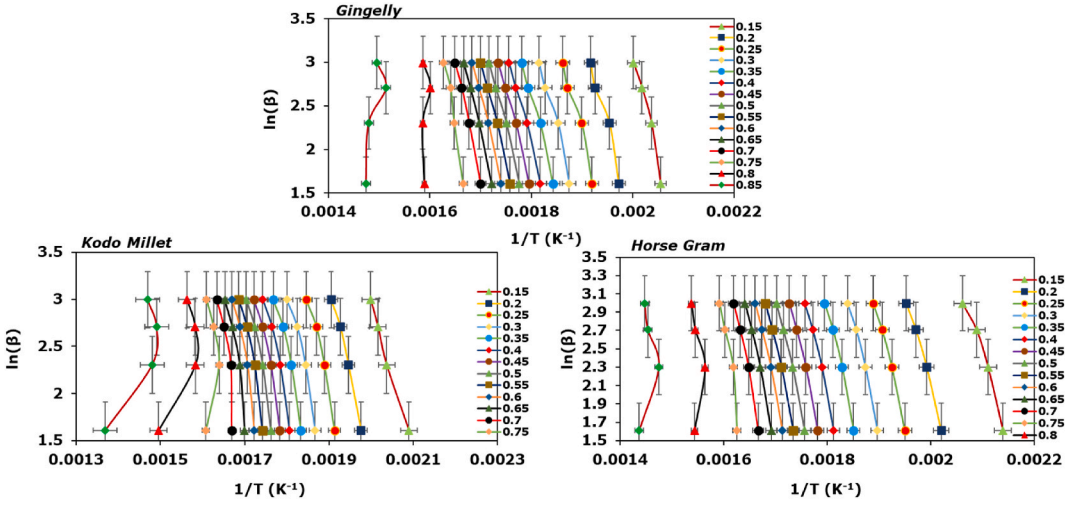

Fig. 2a. Arrhenius plot for biomasses under different iso-conversional model. Fig. 2a FWO model.

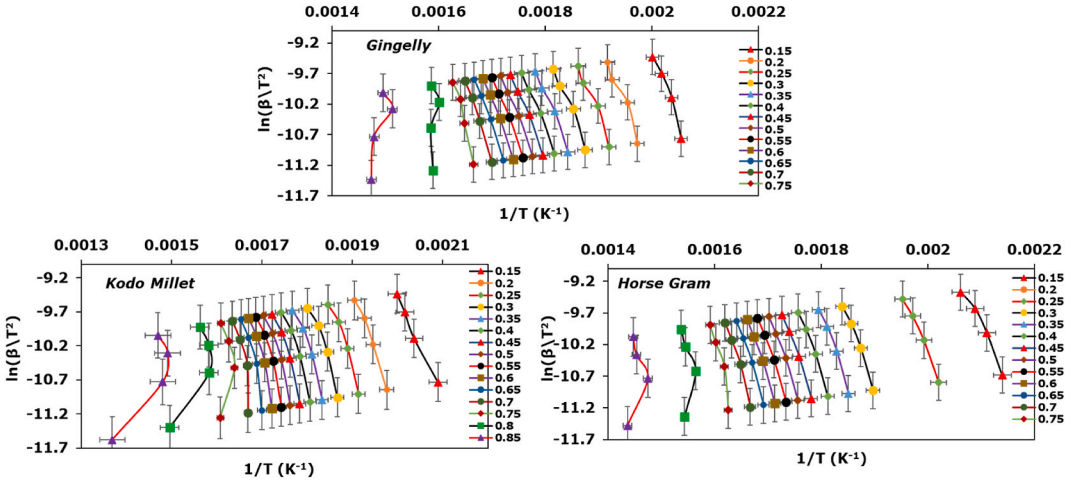

Fig. 2b. KAS model.

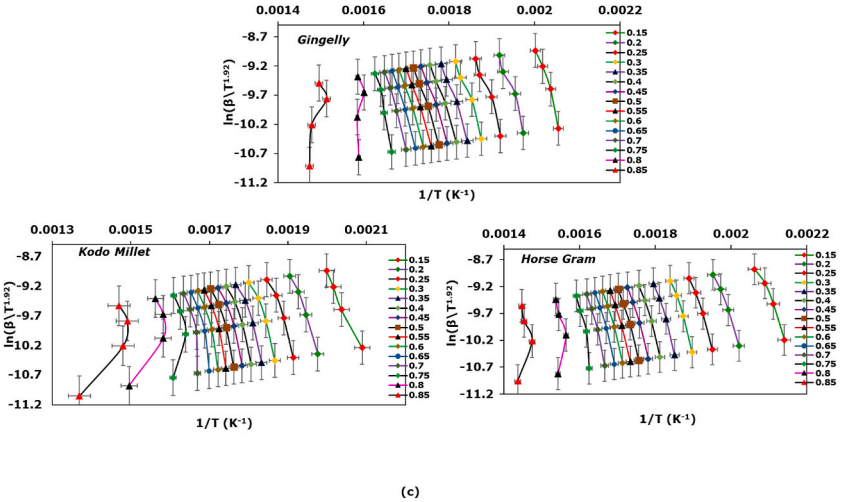

Fig. 2c. Starink model.

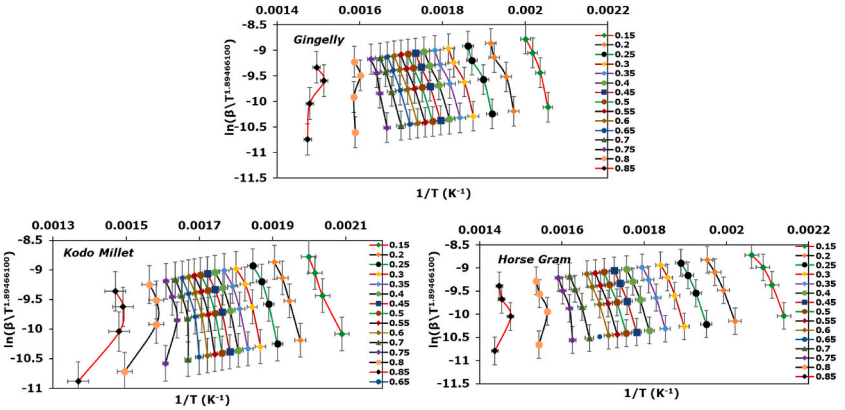

Fig. 2d. Tang model.

Table 4
Kinetic parameters of three types of biomasses under different iso-conversional models.

Method	Conversion	Gingelly			Kodomillet			Horse gram		
		Eα ($kJ.mol^{-1}$)	Aα (S^{-1})	R^2	Eα ($kJ.mol^{-1}$)	Aα (S^{-1})	R^2	Eα ($kJ.mol^{-1}$)	Aα (S^{-1})	R^2
FWO	0.15	135.26	3.1E+15	0.99	115.71	5.18E+12	0.99	193.33	4.53E+21	0.99
	0.20	155.93	8.67E+16	0.98	150.53	8.56E+15	0.97	174.12	3.83E+18	0.98
	0.25	171.49	1.12E+18	0.96	156.12	1.07E+16	0.98	170.41	4.39E+17	0.96
	0.30	183.95	7.55E+18	0.96	157.39	5.62E+15	0.96	169.05	1.14E+17	0.96
	0.35	188.88	8.22E+18	0.97	160.38	5.68E+15	0.96	167.39	3.63E+16	0.97
	0.40	189.78	3.89E+18	0.93	165.13	9.94E+15	0.93	168.51	2.69E+16	0.93
	0.45	192.00	2.98E+18	0.99	170.84	2.3E+16	0.99	171.35	3.23E+16	0.99
	0.50	193.65	2.29E+18	0.98	176.61	5.55E+16	0.98	174.67	4.55E+16	0.98
	0.55	196.43	2.48E+18	0.91	184.89	2.35E+17	0.91	179.03	8.18E+16	0.91
	0.60	200.77	3.85E+18	0.95	197.14	2.34E+18	0.95	184.74	1.97E+17	0.95
	0.65	207.27	9.34E+18	0.96	214.89	7.22E+19	0.96	193.06	8.25E+17	0.96
	0.70	220.92	9.47E+19	0.93	246.46	3.71E+22	0.99	209.88	2.05E+19	0.93
	0.75	281.35	1.33E+25	0.99	36.28	3.406398	0.81	278.03	2.47E+25	0.99
	0.80	98.75	98705916	0.79	85.93	65228.74	0.71	126.06	4.27E+08	0.91
	0.85	74.53	2311.508	0.78	68.03	662.2582	0.70	192.60	3.75E+13	0.97
	Average	179.39	8.88E+23	0.93	152.42	2.48E+21	0.91	183.48	1.65E+24	0.95
KAS	0.15	134.68	1.11E+11	0.97	113.91	2951002	0.97	195.49	2.52E+15	0.99
	0.20	155.99	4.62E+10	0.98	150.12	4.36E+09	0.98	174.94	1.96E+12	0.98
	0.25	172.08	5.6E+11	0.96	155.73	5.07E+09	0.96	170.81	2.12E+11	0.91
	0.30	184.96	3.57E+12	0.96	156.84	2.57E+09	0.96	169.17	5.23E+10	0.95
	0.35	189.92	3.7E+12	0.97	159.85	2.49E+09	0.97	167.26	2.39E+09	0.96
	0.40	190.68	1.67E+12	0.93	164.70	4.23E+09	0.93	168.32	1.16E+10	0.93
	0.45	192.85	1.25E+12	0.99	170.60	9.61E+09	0.99	171.20	1.45E+10	0.99
	0.50	194.46	9.33E+11	0.98	176.56	2.26E+10	0.98	174.60	1.88E+10	0.93
	0.55	197.28	9.78E+11	0.91	185.17	9.3E+10	0.91	179.08	3.31E+10	0.95
	0.60	201.73	1.48E+12	0.95	197.96	9.12E+11	0.95	185.00	7.8E+10	0.96
	0.65	208.45	3.51E+12	0.96	216.52	1.65E+15	0.96	193.65	3.2E+11	0.93
	0.70	222.67	3.46E+13	0.93	249.60	1.37E+16	0.98	211.24	7.77E+12	0.99
	0.75	286.04	4.67E+18	0.97	48.03	9642157	0.87	282.76	9.05E+18	0.91
	0.80	93.57	32.16103	0.75	100.80	2.04E+11	0.73	142.66	1.24E+15	0.97
	0.85	89.40	8.06E+09	0.71	82.80	2.42E+09	0.71	213.33	1.24E+20	0.94
	Average	180.98	3.11E+17	0.92	155.27	1.02E+15	0.92	179.76	8.89E+18	0.95
Starink	0.15	133.91	3.29E+09	0.97	113.31	5207734	0.97	194.25	4.49E+15	0.98
	0.20	155.07	8.25E+10	0.98	149.26	7.79E+09	0.98	173.88	3.5E+12	0.91
	0.25	171.04	1E+12	0.96	154.84	9.14E+09	0.98	169.79	3.8E+11	0.95
	0.30	183.82	6.39E+12	0.96	155.95	4.58E+09	0.96	168.17	9.38E+10	0.96
	0.35	188.76	6.64E+12	0.97	158.92	4.49E+09	0.96	166.28	2.89E+10	0.98
	0.40	189.53	3.01E+12	0.98	163.75	7.67E+09	0.97	167.34	2.09E+10	0.93
	0.45	191.69	2.23E+12	0.96	169.60	1.74E+10	0.98	170.19	2.45E+10	0.99
	0.50	193.28	1.68E+12	0.96	175.53	4.05E+10	0.98	173.57	3.38E+10	0.93
	0.55	196.08	1.76E+12	0.97	180.07	1.68E+11	0.91	178.03	5.96E+10	0.95
	0.60	200.50	2.68E+12	0.93	196.76	1.64E+12	0.95	183.90	1.41E+11	0.96
	0.65	207.18	6.33E+12	0.96	215.19	4.96E+13	0.96	192.50	5.78E+11	0.93
	0.70	221.29	6.27E+13	0.93	248.00	2.48E+16	0.98	209.95	1.4E+13	0.99
	0.75	284.16	8.46E+18	0.97	47.25	5323574	0.85	280.91	1.64E+19	0.91
	0.80	93.24	58.44905	0.77	99.59	1.12E+11	0.74	141.93	6.85E+14	0.97
	0.85	88.25	4.41E+09	0.73	81.69	1.32E+09	0.78	212.45	6.82E+19	0.94
	Average	179.85	5.64E+17	0.93	153.98	1.66E+15	0.93	185.54	5.64E+18	0.95
Tang	0.15	134.89	3.94E+09	0.98	114.16	6234790	0.99	195.62	5.39E+15	0.97
	0.20	156.13	9.91E+10	0.91	150.34	9.38E+09	0.98	175.12	4.2E+12	0.98
	0.25	172.27	1.2E+12	0.95	155.95	1.1E+10	0.91	171.01	4.57E+11	0.96
	0.30	185.13	7.68E+12	0.96	157.08	5.54E+09	0.95	169.38	1.13E+11	0.96
	0.35	190.11	7.99E+12	0.98	160.07	5.43E+09	0.96	167.48	3.48E+10	0.97
	0.40	190.88	3.62E+12	0.93	164.94	9.24E+09	0.93	168.55	2.51E+10	0.98
	0.45	193.06	2.69E+12	0.99	170.83	2.07E+10	0.99	171.43	2.94E+10	0.96
	0.50	194.66	2.03E+12	0.93	176.89	4.92E+10	0.96	174.82	4.05E+10	0.96
	0.55	197.48	2.13E+12	0.97	185.40	2.05E+11	0.97	179.31	7.18E+10	0.95
	0.60	201.93	1.35E+16	0.93	198.17	1.98E+12	0.93	185.22	1.69E+11	0.96
	0.65	208.05	7.57E+12	0.96	216.71	6E+13	0.96	193.87	6.97E+11	0.93
	0.70	222.86	7.55E+13	0.93	249.74	2.99E+16	0.93	211.44	1.69E+13	0.99
	0.75	286.14	1.02E+19	0.97	47.44	4415605	0.86	282.87	1.97E+19	0.91
	0.80	93.98	70.63003	0.72	100.11	9.21E+10	0.72	141.93	5.67E+14	0.97
	0.85	88.69	3.64E+09	0.70	82.08	1.1E+09	0.74	212.45	5.62E+19	0.94
	Average	181.08	6.81E+17	0.92	155.32	2E+15	0.91	186.70	5.06E+18	0.95

wall polymers i.e., cellulose and hemicellulose. After 75 % conversion level, all the major polymers would have been degraded and hence, it is apparent that the energy input requirements will be considerably lower at higher conversion. Similar pattern was also noticed in case of gingelly biomass. The (Table 5) provides a comparative estimate of activation energy for different biomasses under different models. The estimates of Eα for little millet was around as 192 kJ/mol (FWO and KAS), whereas for sunflower, the Eα was observed as 166 kJ/mol (FWO) and 162 kJ/mol (KAS) [2]. The apparent Eα was found as 178 kJ/mol and 173 kJ/mol under Starink and Friedman, respectively for finger millet [32] and 150 kJ/mol under FWO for pearl millet [33]. The apparent Eα was determined around 231 kJ/mol (for particle size 0.25–0.71 mm) for ground nut shell [39]. The apparent Eα was determined as 203 kJ/mol for castor oil under both KAS and FWO [38]. Hence, the mean Eα values of gingelly biomass is comparably lower to various oilseed crops like ground nut and castor and comparable with the sunflower (*Helianthus annus*) indicating the desirability of gingelly biomass for potential feedstocks.

The figure (Fig. 4(a–d)) depicted fluctuations of Eα estimates with varied conversion level (15–85 %). With the rise in "α" from 15 % to 75 %, the Eα values escalated accordingly for gingelly and kodo millet biomasses. For gingelly biomass, the Aα values of 10^{15} to 10^{25}, 10^{11} to 10^{18}, 10^{9} to 10^{18} and 10^{9} to 10^{19} under FWO, KAS, S and T, respectively were observed. For kodo, the Aα values of 10^{12} to 10^{22}, 10^{9} to 10^{16}, 10^{9} to 10^{16} and 10^{9} to 10^{16} under FWO, KAS, S and T, respectively were calculated. For horse gram, the Aα values of 10^{8} to 10^{21}, 10^{9} to 10^{20}, 10^{1} to 10^{19} and 10^{10} to 10^{19} under FWO, KAS, S and T, respectively were determined. Gradual rise in pre-exponential factors with the heating rate is essentially ascribed due to higher collision frequency of the particles. Changes in frequency factor estimates with the "α" is principally ascribed due to the existence of multi-step higher order reaction mechanism during the disintegration of biomass [41]. Low estimates of Aα ($<10^{9}$ s^{-1}) thus generated, suggest the ongoing reaction processes to be less reactive with the existence of surface reaction only. While, higher Aα ($>10^{9}$ s^{-1}) estimate, suggests the kodo millet to be highly reactive with simplex complex type reactions [5]. Frequency factor deals with the frequency of molecules that collide in the correct orientation and with high energy to initiate a reaction. Hence, a higher value of this factor is desirable to initiate pyrolysis process for production of biofuels.

3.6. Analysis of thermodynamic parameters

Thermodynamic parameters viz., ΔHα, ΔGα and ΔSα estimates were generated by employing several mathematical expressions and approximations in Table 6 as suggested by various authors (Eqs. (8)–(10)). Horse gram biomass exhibited highest ΔHα estimates (178.91 kJ/mol) whereas kodo exhibited the lowest estimate (147.83 kJ/mol) under FWO. The mean estimates of ΔHα were 174.81 (FWO), 170.22 (KAS), 169.17 (S) and 170.40 (T) kJ/mol for the gingelly biomass. The mean estimates of ΔHα were 147.83 (FWO), 148.81 (KAS),147.93 (S) and 149.04 (T) kJ/mol for kodo milley biomass, while for horse gram biomass, mean estimates of ΔHα were 178.91 (FWO), 169.61 (KAS),168.56 (S) and 168.81 (T) kJ/mol. The mean values of ΔHα for sunflower branch were 161 (FWO), 158 (KAS), 160 (S) and 158(T) kJ/mol [2]. For gingelly and kodo millet, the ΔHα calculates increased with the rise in conversion, thereby suggesting the endothermic behaviour of thermal disintegration the biomass. During pyrolysis, the breaking of chemical bonds in the biomass requires an input of energy making it an endothermic process. This energy is typically supplied through the heating of biomass, the endothermic nature of pyrolysis helps in the conversion of complex organic molecules into simpler compounds like bio-oils, which can then be further processed into liquid biofuels such as ethanol and biodiesel. The difference between ΔHα and Eα estimates were found to be minimal (3–4 kJ/mol), indicating the potentiality of the three biomass as potential feedstock. Hence, an additional low level (3–4 kJ/mol) of energy inputs will be necessitated in the due processes [42]. The ΔGα estimates under KAS was determined as 185.84 kJ/mol for gingelly, 191 kJ/mol for kodo millet and 191.53 kJ/mol for horse gram. The ΔGα estimates under Starink was determined as 184.54 kJ/mol for gingelly, 187.61 kJ/mol for kodo and 186.84 kJ/mol for horse gram. The positive values of ΔGα indicates the non-spontaneous nature of reaction, requiring external energy for the reaction to proceed. A lower value of this parameter is essential for biofuel purpose. The ΔGα values obtained for gingelly is less compared to other two biomasses. Hence, gingelly is a better biofuel feedstock as compared to kodo millet and horse gram. These + ve and -ve ΔSα estimates suggest the multi-step reaction mechanisms operating during the gingelly biomass combustion [4]. Mean estimates of ΔSα (entropy) was recorded as −0.03, −0.07 and −0.03 under KAS and 0.06, 0.01 and 0.07 under OFW for gingelly, kodo and horse gram, respectively. Various

Table 5
Comparative estimates of activation energy of different biomasses.

SI.No	Biomass	Activation energy	Reference(s)
1	Little Millet	192 kJ/mol (FWO and KAS)	[2]
2	Sunflower	166 kJ/mol (FWO) and 162 kJ/mol (KAS)	[2]
3	Finger Millet	178 kJ/mol (Starink) and 173 kJ/mol (Friedman)	[32]
4	Pearl Millet	150 kJ/mol under FWO	[33]
5	Rice	175.50(FWO), 174.93(KAS),174.14(Starink) and 175.17(Tang)	[42]
6	Ground Nut Shell	231 kJ/mol	[39]
7	Castor Oil	203 kJ/mol KAS and FWO	[38]
8	Banana	206.12 kJ/mol (FWO), 207.19 kJ/mol (KAS), 205.9 kJ/mol (Starink) and 207.37 kJ/mol (Tang)	[3]
9	Rice	173.40 kJ/mol (FWO)	[1]
10	Banyan tree	73.03 kJ/mol (KAS) and 79.74 kJ/mol (FWO)	[19]
11	Maple Leaf	91.50 kJ/mol (FWO), 75.31 kJ/mol (Friedman), 75.83 kJ/mol (KAS)	[20]
12	Cotton	226 kJ/mol (KAS & FWO)	[21]

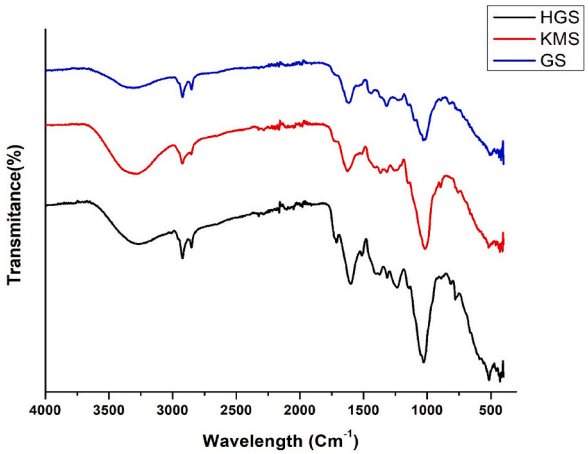

Fig. 3. FTIR curve of stem biomass.

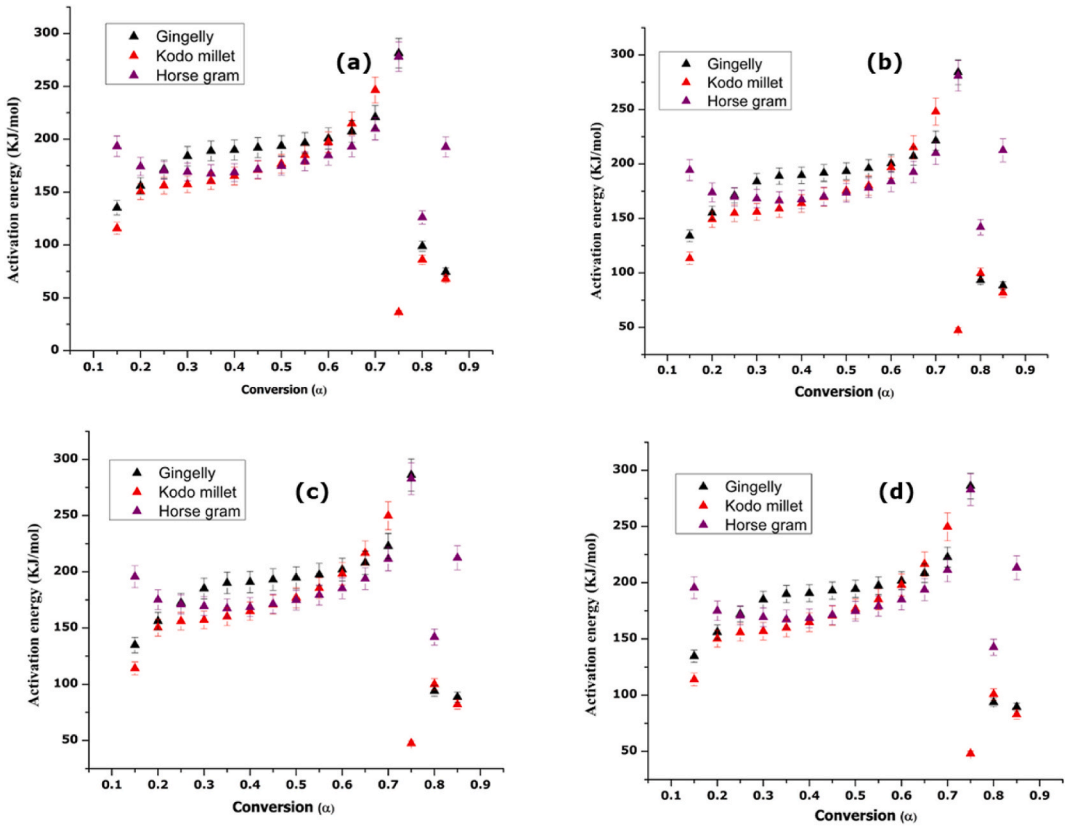

Fig. 4. Variation in activation energy with conversion for FWO (a), KAS (b), Starink (c) and Tang (d).

authors in different biomass such as castor [26], rice [9], little millet and sunflower [2], have observed similar findings. Differences in the thermodynamics parameters is different in the three types of biomasses studied which probably is due to different biochemical constitutions (cell wall polymers).

3.7. Reaction mechanism study

Reaction mechanism involved in thermal disintegration of three types of biomass was explored by master plot analysis (Fig. 5). Master plots basically encompasses various theoretical and experimental curves, which are generated by equating complex

Table 6
Thermodynamic parameters of three types of biomasses under different iso-conversional models.

Method	Conversion	Gingelly			Kodo millet			Horse gram		
		ΔHα (kJ. mol^{-1})	ΔGα (kJ. mol^{-1})	ΔSα (kJ. mol^{-1})	ΔHα (kJ. mol^{-1})	ΔGα (kJ. mol^{-1})	ΔSα (kJ. mol^{-1})	ΔHα (kJ. mol^{-1})	ΔGα (kJ. mol^{-1})	ΔSα (kJ. mol^{-1})
FWO	0.15	131.47	113.46	0.03	111.78	118.38	−0.01	189.41	115.43	0.15
	0.20	151.91	119.70	0.06	146.41	123.05	0.04	170.02	121.76	0.09
	0.25	167.33	123.50	0.08	151.88	127.01	0.04	166.19	125.77	0.07
	0.30	179.68	126.62	0.09	153.05	130.45	0.04	164.73	129.24	0.06
	0.35	184.50	129.87	0.09	155.96	132.97	0.04	162.99	131.92	0.05
	0.40	185.31	132.99	0.09	160.64	134.87	0.04	164.04	133.92	0.05
	0.45	187.45	135.42	0.09	166.30	136.45	0.05	166.83	135.56	0.05
	0.50	189.03	137.53	0.08	172.01	137.84	0.05	170.10	136.98	0.05
	0.55	191.75	139.29	0.08	180.25	139.06	0.07	174.41	138.28	0.06
	0.60	196.03	140.92	0.09	192.45	140.12	0.08	180.07	139.53	0.06
	0.65	202.48	142.50	0.10	210.15	141.06	0.11	188.34	140.67	0.08
	0.70	216.06	144.08	0.11	241.66	141.81	0.16	205.11	141.60	0.10
	0.75	276.40	144.58	0.21	31.40	177.54	−0.23	273.17	140.67	0.21
	0.80	93.63	159.15	−0.10	80.87	182.58	−0.16	121.01	178.19	−0.09
	0.85	69.10	196.74	−0.18	62.62	196.51	−0.19	187.19	187.29	−0.0001
	Average	174.81	139.09	0.06	147.83	141.51	0.01	178.91	138.57	0.07
KAS	0.15	130.89	151.67	−0.04	109.98	173.05	−0.12	191.57	173.92	0.03
	0.20	151.97	177.75	−0.05	146.00	182.20	−0.07	170.84	181.87	−0.02
	0.25	167.92	184.38	−0.03	151.49	188.26	−0.06	166.59	187.42	−0.03
	0.30	180.69	189.81	−0.01	152.50	193.22	−0.07	164.85	192.35	−0.05
	0.35	185.54	194.84	−0.01	155.43	197.13	−0.07	162.86	204.54	−0.07
	0.40	186.21	199.32	−0.02	160.21	200.22	−0.07	163.85	199.16	−0.06
	0.45	188.30	203.08	−0.02	166.06	202.89	−0.06	166.68	201.48	−0.06
	0.50	189.84	206.25	−0.02	171.96	205.33	−0.05	170.03	204.07	−0.05
	0.55	192.60	209.06	−0.02	180.53	207.74	−0.04	174.46	206.29	−0.05
	0.60	196.99	211.73	−0.02	193.27	210.12	−0.02	180.33	208.54	−0.04
	0.65	203.66	214.51	−0.01	211.78	193.31	0.03	188.93	210.82	−0.03
	0.70	217.81	217.77	0.0006	244.88	216.02	0.04	206.47	213.47	−0.01
	0.75	281.09	222.76	0.09	43.15	116.79	−0.12	277.90	217.32	0.09
	0.80	88.40	230.36	−0.22	95.74	121.86	−0.04	137.61	119.7	0.02
	0.85	83.97	129.90	−0.06	77.39	129.64	−0.07	207.92	126.82	0.11
	Average	170.22	185.84	−0.03	148.81	191.00	−0.07	169.61	191.53	−0.03
STARINK	0.15	130.12	164.24	−0.07	109.38	170.22	−0.12	190.33	170.43	0.04
	0.20	151.05	174.50	−0.04	145.14	178.95	−0.06	169.78	178.44	−0.01
	0.25	166.88	180.92	−0.02	150.60	184.87	−0.06	165.57	183.95	−0.03
	0.30	179.55	186.18	−0.01	151.61	189.81	−0.07	163.85	188.83	−0.04
	0.35	184.38	191.12	−0.01	154.50	193.59	−0.07	161.88	192.59	−0.05
	0.40	185.06	195.56	−0.01	159.26	196.60	−0.06	162.87	195.57	−0.05
	0.45	187.14	199.27	−0.02	165.06	199.20	−0.06	165.67	198.09	−0.05
	0.50	188.66	202.35	−0.02	170.93	201.63	−0.05	169.00	200.35	−0.05
	0.55	191.40	205.10	−0.02	175.43	199.91	−0.04	173.41	202.52	−0.05
	0.60	195.76	207.71	−0.02	192.07	206.15	−0.02	179.23	204.69	−0.04
	0.65	202.39	210.42	−0.01	210.45	208.59	0.003	187.78	206.89	−0.03
	0.70	216.43	213.51	0.004	243.2	211.57	0.05	205.18	209.36	−0.007
	0.75	279.21	217.93	0.09	42.37	118.91	−0.12	276.05	212.59	0.10
	0.80	88.12	226.97	−0.21	94.53	123.67	−0.04	136.88	121.97	0.02
	0.85	82.82	132.02	−0.07	76.28	131.79	−0.08	207.04	129.19	0.11
	Average	169.17	184.54	−0.03	147.93	187.61	−0.07	168.56	186.84	−0.03
TANG	0.15	131.10	164.55	−0.07	110.22	170.36	−0.12	191.70	171.09	0.04
	0.20	152.11	174.83	−0.04	146.22	179.27	−0.06	171.02	178.93	−0.01
	0.25	168.11	181.39	−0.02	151.71	185.20	−0.06	166.79	184.39	−0.03
	0.30	180.86	186.70	−0.01	152.74	190.12	−0.06	165.06	189.24	−0.04
	0.35	185.73	191.66	−0.01	155.65	193.91	−0.06	163.08	192.98	−0.05
	0.40	186.41	196.08	−0.01	160.45	196.95	−0.06	164.08	195.95	−0.05
	0.45	188.51	199.79	−0.01	166.29	199.63	−0.05	166.91	198.50	−0.05
	0.50	190.04	202.87	−0.02	172.29	202.10	−0.05	170.25	200.77	−0.05
	0.55	192.80	205.63	−0.02	180.76	204.31	−0.04	174.69	202.94	−0.04
	0.60	197.19	168.82	0.04	193.48	206.68	−0.02	180.55	205.14	−0.04
	0.65	203.26	210.43	−0.01	211.97	209.21	0.004	189.15	207.38	−0.03
	0.70	218.00	214.18	0.006	244.94	212.40	0.05	206.67	209.96	−0.005
	0.75	281.19	218.98	0.10	42.56	120.01	−0.12	278.01	213.64	0.10
	0.80	88.86	226.75	−0.21	95.05	125.19	−0.04	136.88	122.93	0.02
	0.85	83.26	133.50	−0.07	76.67	133.19	−0.08	207.04	130.24	0.11
	Average	170.40	185.00	−0.02	149.04	187.92	−0.07	169.81	187.30	−0.03

mathematical equations and approximations (Eqs. (11) and (12)). Under the current investigation, three experimental curves of three concerned biomasses were tallied with various theoretical curves that corresponds to a different solid-state function. The categorization of reaction types implicated in the thermal disintegration of cell wall polymers can be deduced by scrutinizing the proximity between the experimental curve and theoretical counterparts across distinct levels of conversion. in the present investigation, the reaction mechanism analysis was carried out by taking conversion from 0.2 to 0.7. For gingelly biomass, up to 40 % disintegration of biomass, the reaction mechanism was observed to be R1 (limiting surface reaction-one dimension). At elevated conversion levels, reaching up to 60 %, the observed reaction mechanism became notably complex one. This was evident as the experimental curve intersected multiple theoretical curves, encompassing R2 (limiting surface reaction - two dimensions), F3 (chemical reaction - third order), and D2 (two-way transport diffusion model). Particularly at these advanced conversion levels, the experimental curve exhibited the closest alignment with F1, a model associated with chemical reactions of third-order nature. Similar pattern was followed for the kodo biomass with respect to the reaction mechanism. The experimental curve for horse gram was observed to cut through several solid-state reaction curves such as D2 (two-way transport diffusion model) and F3 (chemical reaction-third order) before touching F1 (chemical reaction-first order). Consequently, the aforementioned results lead to the inference that the reaction mechanism underlying thermal disintegration constitutes a intricate phenomenon. By understanding the individual steps and intermediates involved in the reaction mechanisms, it enables to optimise reaction conditions such as temperature, pressure, pH and biocatalysts concentrations. This optimisation helps to improve bioethanol recovery.

3.8. Ethanol production in a laboratory bioreactor via SSF

A composite microwave-alkali-acid pre-treatment technique is utilized to extract ethanol from gingelly, kodo millet, and horse gram straw [43] (Table 7). Gingelly biomass yielded an ethanol titer of 24.8 g/L after 24 h, resulting in a volumetric ethanol productivity of 1.03 g/L/h and an ethanol yield of 0.36 g/g. For kodo millet, the ethanol titer reached 22.9 g/L, accompanied by a volumetric ethanol productivity of 0.98 g/L/h and an ethanol yield of 0.35 g/g. For horse gram, the ethanol titer value, volumetric ethanol productivity and ethanol yield were 18.75 g/L, 0.95 g/L/h and 0.29 g/g, respectively. Hence, it is apparent that gingelly has got the highest bioenergy potential among the three types of biomasses, which is closely followed by kodo millet.

4. Conclusion

The existence of significant amount of cellulose (38.07 %), volatiles (75.19 %), calorific value (avg. 16.98 MJ/kg) in the gingelly biomass, demonstrates the effectiveness of the biomass for utilization as raw material in diverse industrial applications. The mean estimates of Eα were lower for kodo millet (approx. 150 kJ/mole), followed by gingelly (approx. 178 kJ/mole) and horse gram (approx. 180 kJ/mole). The mean estimates of ΔHα were 174.81 (FWO), 170.22 (KAS), 169.17 (S) and 170.40 (T) kJ/mol for the gingelly biomass. The mean estimates of ΔHα were 147.83 (FWO), 148.81 (KAS), 147.93 (S) and 149.04 (T) kJ/mol for kodo millet biomass, while for horse gram biomass, mean estimates of ΔHα were 178.91 (FWO), 169.61 (KAS), 168.56 (S) and 168.81 (T) kJ/mol. The minor difference of 3–4 kJ/mole between Aα and Hα, signifies the viability of the thermal disintegration process. Upon interpreting the master plot, optimisation of reaction conditions such as temperature, pressure, pH and biocatalysts concentrations was performed for improved bioethanol recovery. The gingelly biomass records a broad peak of higher intensities at the 3300-3500 cm^{-1} wavelength range as compared to other two biomasses. Interestingly, gingelly exhibited highest cellulose accumulation (38.07 %) along with highest ethanol recovery (0.36 g/g) as compared to other biomasses. Hence, it is apparent that gingelly has got the highest bioenergy potential among the three types of biomasses.

Funding

This research didn't receive any specific grant from funding agencies in the public, commercial or not-for-profit sectors.

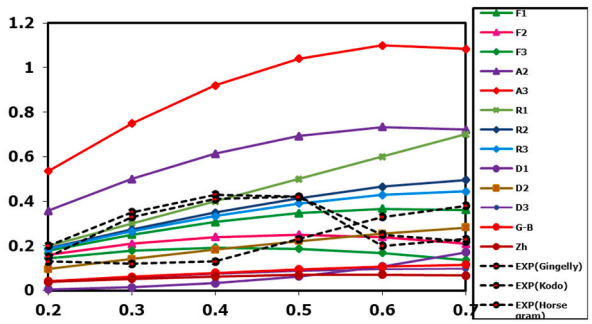

Fig. 5. Master plot analysis in three different types of biomass.

Table 7
Ethanol production using pre-treated gingelly, kodo millet and horse gram stem biomass as feedstocks.

Biomass	Ethanol concentration (g/L)	Volumetric ethanol productivity (g/L/h)	Ethanol yield (g/g)
Gingelly	24.8	1.03	0.36
Kodo millet	22.9	0.98	0.35
Horse gram	18.75	0.95	0.29

Data availability

The data that has been used is available on request from the corresponding author.

CRediT authorship contribution statement

Spandan Nanda: Writing- original Draft, Conceptualization, Investigation, Methodology, Software. **Abinash Mishra:** Editing-original draft, Data curation, Software. **Amrita Priyadarsini:** Visualization, Data curation. **Tanya Barpanda:** Formal analysis. **Amiya Kumar Baral:** Formal analysis. **Supriya Jena:** Formal analysis. **Pradip Kumar Jena:** Investigation, Formal Analysis, supervision. **Bipranarayan Mallick:** Formal analysis. **Manasi Dash:** Formal Analysis, Conceptualization, Methodology, Supervision, Software. **Nandita Swain:** Supervision. **Nitish Kumar Jena:** Data curation. **Mahendra Kumar Mohanty:** Data curation.

Declaration of competing interest

The authors declare that they have no known competing financial interests or personal relationships that could have appeared to influence the work reported in this paper.

Acknowledgement

Authors acknowledge the Central Instrumentation Facility, OUAT and BPCL -BIOFUEL Project, OUAT, Bhubaneswar, India for technical support. This study is a part of the Ph.D. Research work of first author.

Appendix A. Supplementary data

Supplementary data to this article can be found online at https://doi.org/10.1016/j.heliyon.2024.e36946.

References

[1] S. Nanda, B. Swain, A. Priyadarsini, A. Mishra, M.R. Parida, P.K. Jena, M. Dash, Thermodynamic, spectroscopic, and molecular characterization of rice straw biomass for use as biofuel feedstock, Can. J. Chem. Eng 102 (5) (2024) 1842–1851.
[2] A. Mishra, S. Nanda, M.R. Parida, P.K. Jena, S.K. Dwibedi, S.M. Samantaray, M. Dash, A comparative study on pyrolysis kinetics and thermodynamic parameters of little millet and sunflower branchs biomass using thermogravimetric analysis, Bioresour. Technol. 367 (2023) 128231.
[3] A. Priyadarsini, B. Swain, A. Mishra, S. Nanda, M. Dash, N. Swain, M.K. Mohanty, Study on biofuel efficiency of tropical banana leaf biomass using spectroscopy, kinetic and thermodynamic parameters, Bioresour. Technol. Rep. 23 (2023) 101522.
[4] I. Ali, H. Bahaitham, R. Naebulharam, A comprehensive kinetics study of coconut shell waste pyrolysis, Bioresour. Technol. 235 (2017) 1–11, https://doi.org/10.1016/j.biortech.2017.03.089.
[5] V. Dhyani, J. Kumar, T. Bhaskar, Thermal decomposition kinetics of sorghum straw via thermogravimetric analysis, Bioresour. Technol. 245 (2017) 1122–1129, https://doi.org/10.1016/j.biortech.2017.08.189.
[6] D. Chen, Y. Wang, Y. Liu, K. Cen, X. Cao, Z. Ma, Y. Li, Comparative study on the pyrolysis behaviors of rice straw under different washing pretreatments of water, acid solution, and aqueous phase bio-oil by using TG-FTIR and Py-GC/MS, Fuel 252 (2019) 1–9, https://doi.org/10.1016/j.fuel.2019.04.086.
[7] G.K. Gupta, M.K. Mondal, Kinetics and thermodynamic analysis of maize cob pyrolysis for its bioenergy potential using thermogravimetric analyzer, J. Therm. Anal. Calorim. 137 (4) (2019) 1431–1441, https://doi.org/10.1007/s10973-019-08053-7.
[8] J.K. Sarkar, Q. Wang, Characterization of pyrolysis products and kinetic analysis of waste jute stick biomass, Processes 8 (7) (2020) 837, https://doi.org/10.3390/pr8070837.
[9] S. Singh, T. Patil, S.P. Tekade, M.B. Gawande, A.N. Sawarkar, Studies on individual pyrolysis and co-pyrolysis of corn cob and polyethylene: thermal degradation behavior, possible synergism, kinetics, and thermodynamic analysis, Sci. Total Environ. 783 (2021) 147004, https://doi.org/10.1016/j.scitotenv.2021.147004.
[10] D.B. Pal, A.K. Tiwari, N. Srivastava, A. Hashem, Abd Allah, E.F., Thermal studies of biomass obtained from the seeds of Syzygium cumini and Cassia fistula L. and peel of Cassia fistula L. fruit, Biomass Convers. Biorefin 1–12 (2021), https://doi.org/10.1007/s13399-021-01492-z.
[11] P.N. Dave, R. Sirach, R. Thakkar, S. Chaturvedi, Thermal decomposition of 3-Nitro-1, 2, 4-Triazole-5-one (NTO) and Nanosize NTO Catalyzed by NiFe2O4, Arabian J. Sci. Eng. 48 (1) (2023) 467–474.
[12] D. Myint, S.A. Gilani, M. Kawase, K.N. Watanabe, Sustainable sesame (Sesamum indicum L.) production through improved technology: an overview of production, challenges, and opportunities in Myanmar, Sustainability 12 (9) (2020) 3515.
[13] K.F. Dossa, A.A. Enete, Y.E. Miassi, A.O. Omotayo, Economic analysis of gingelly (Sesamum indicum L.) production in Northern Benin, Frontiers in Sustainable Food Sybranchs 6 (2023) 1015122.
[14] C. Li, Y. Sun, S. Zhang, Y. Wang, J. Xiang, S. Hu, X. Hu, Pyrolysis of sesame residue: Evolution of the volatiles and structures of biochar versus temperature, Environ. Technol. Innovat. 24 (2021) 101859.
[15] A.N. Sanjay, G. Basarkar, V. Buchake, Millets: an overview-A treatise on healthy option in daily diet, J. Pharmacogn. Phytochem. 11 (3) (2022) 177–185.

[16] K. Kiranmai, L.R. Gunupuru, A. Nareshkumar, V.A. Reddy, U. Lokesh, M. Pandurangaiah, C. Sudhakar, Expression Analysis of WRKY Transcription Factor Genes in Response to Abiotic Stresses in Horsegram (Macrotyloma Uniflorum (Lam.) Verdc.), 2016.
[17] A. Bhartiya, J.P. Aditya, L. Kant, Nutritional and remedial potential of an underutilized food legume horsegram (Macrotyloma uniflorum): a review, JAPS: Journal of Animal & Plant Sciences 25 (4) (2015).
[18] A. Sahoo, S. Kumar, J. Kumar, T. Bhaskar, A detailed assessment of pyrolysis kinetics of invasive lignocellulosic biomasses (Prosopis juliflora and Lantana camara) by thermogravimetric analysis, Bioresour. Technol. 319 (2021) 124060.
[19] T. Rasool, S. Kumar, Kinetic and thermodynamic evaluation of pyrolysis of plant biomass using TGA, Mater. Today: Proc. 21 (2020) 2087–2095.
[20] M.S. Ahmad, J.J. Klemeš, H. Alhumade, A. Elkamel, A. Mahmood, B. Shen, A. Bokhari, Thermo-kinetic study to elucidate the bioenergy potential of Maple Leaf Waste (MLW) by pyrolysis, TGA and kinetic modelling, Fuel 293 (2021) 120349.
[21] R.N. Mandapati, P.K. Ghodke, Kinetics of pyrolysis of cotton stalk using model-fitting and model-free methods, Fuel 303 (2021) 121285.
[22] T. Ozawa, A new method of analyzing thermogravimetric data, Bull. Chem. Soc. Jpn. 38 (11) (1965) 1881–1886, https://doi.org/10.1246/bcsj.38.1881.
[23] T. Akahira, T. Sunose, Method of determining activation deterioration constant of electrical insulating materials, Res Rep Chiba Inst Technol (Sci Technol). 16 (1971) 22–31.
[24] M.J. Starink, The determination of activation energy from linear heating rate experiments: a comparison of the accuracy of isoconversion methods, Thermochim. Acta 404 (1–2) (2003) 163–176, https://doi.org/10.1016/S0040-6031(03)00144-8.
[25] W. Tang, Y. Liu, H. Zhang, C. Wang, New approximate formula for Arrhenius temperature integral, Thermochim. Acta 408 (1–2) (2003) 39–43, https://doi.org/10.1016/S0040-6031(03)00310-1.
[26] R. Kaur, P. Gera, M.K. Jha, T. Bhaskar, Pyrolysis kinetics and thermodynamic parameters of castor (Ricinus communis) residue using thermogravimetric analysis, Bioresour. Technol. 250 (2018) 422–428, https://doi.org/10.1016/j.biortech.2017.11.077.
[27] P. Binod, R. Sindhu, R.R. Singhania, S. Vikram, L. Devi, S. Nagalakshmi, A. Pandey, Bioethanol production from rice straw: an overview, Bioresour. Technol. 101 (13) (2010) 4767–4774.
[28] A. Mishra, M. Dash, T. Barpanda, A. Sibadatta, P. Sahu, P. Sahu, M.K. Mohanty, A comprehensive molecular, biochemical, histochemical, and spectroscopic characterization of early and medium duration rice genotypes investigating dry matter accumulation efficiencies, Appl. Biochem. Biotechnol. (2024) 1–17.
[29] A. Priyadarsini, C. Mohanty, S. Nanda, A. Mishra, N. Das, N. Swain, P.K. Jena, Synergistic cobalt oxide/reduced graphene oxide/biochar nano-composite catalyst: harnessing the power of the catalyst for sustainable remediation of organic dyes and chromium (VI), RSC Adv. 14 (14) (2024) 10089–10103.
[30] M. Kumar, S.K. Shukla, S.N. Upadhyay, P.K. Mishra, Analysis of thermal degradation of banana (Musa balbisiana) trunk biomass waste using iso-conversional models, Bioresour. Technol. 310 (2020) 123393, https://doi.org/10.1016/j.biortech.2020.123393.
[31] R.K. Mishra, K. Mohanty, Characterization of non-edible lignocellulosic biomass in terms of their candidacy towards alternative renewable fuels, Biomass Conversion and Biorefinery 8 (4) (2018) 799–812, https://doi.org/10.1007/s13399-018-0332-8.
[32] V.K. Vikraman, D.P. Kumar, G. Boopathi, P. Subramanian, Kinetic and thermodynamic study of finger millet straw pyrolysis through thermogravimetric analysis, Bioresour. Technol. 342 (2021) 125992, https://doi.org/10.1016/j.biortech.2021.12599.
[33] P. Kumar, P.M.V. Subbarao, L.D. Kala, V.K. Vijay, Thermogravimetry and associated characteristics of pearl millet cob and eucalyptus biomass using differential thermal gravimetric analysis for thermochemical gasification, Therm. Sci. Eng. Prog. 26 (2021) 101104, https://doi.org/10.1016/j.tsep.2021.101104.
[34] X. Huang, J.P. Cao, X.Y. Zhao, J.X. Wang, X. Fan, Y.P. Zhao, X.Y. Wei, Pyrolysis kinetics of soybean straw using thermogravimetric analysis, Fuel 169 (2016) 93–98, https://doi.org/10.1016/j.fuel.2015.12.011.
[35] V. Dhyania, J. Kumar, T. Bhaskar, A comparative study of thermal decomposition kinetics of cellulose, hemicellulose, and lignin, Cellulose 95 (5.0) (2020) 1, 0.
[36] X. Chen, J. Yu, Z. Zhang, C. Lu, Study on structure and thermal stability properties of cellulose fibers from rice straw, Carbohydr. Polym. 85 (1) (2011) 245–250, https://doi.org/10.1016/j.carbpol.2011.02.022.
[37] T. Gerci, Influence of process Variables on oils from Tire pyrolysis and Hydropyrolysis in a Swept fixed bed reactor, Energy Fuel. 14 (2000) 3545–3550.
[38] H. Li, S. Niu, C. Lu, Thermal characteristics and kinetic calculation of castor oil pyrolysis, Procedia Eng. 205 (2017) 3711–3716.
[39] D.K. Ojha, V.S.P. Kumar, R. Vinu, Analytical pyrolysis of bagasse and groundnut shell briquettes: kinetics and pyrolysate composition studies, Bioresour. Technol. Rep. 15 (2021) 100784.
[40] R. Sirach, P.N. Dave, Thermal and bisphenol-A adsorption properties of a zinc ferrite/β-cyclodextrin polymer nanocomposite, RSC Adv. 13 (32) (2023) 21991–22006.
[41] V. Dhyani, T. Bhaskar, A comprehensive review on the pyrolysis of lignocellulosic biomass, Renew. Energy 129 (2018) 695–716, https://doi.org/10.1016/j.renene.2017.04.035.
[42] A. Mishra, T.K. Mishra, S. Nanda, P.K. Jena, S.K. Dwibedi, B. Jena, M. Dash, Bioenergy potential of different varieties of paddy straw biomass, Bioresour. Technol. Rep. 20 (2022) 101229.
[43] N. Akhtar, D. Goyal, A. Goyal, Characterization of microwave-alkali-acid pre-treated rice straw for optimization of ethanol production via simultaneous saccharification and fermentation (SSF), Energy Convers. Manag. 141 (2017) 133–144.